Hand-feel soil texture and particle-size distribution in central France. Relationships and implications

Anne Richer-De-Forges, Dominique Arrouays, Songchao Chen, Mercedes Román Dobarco, Zamir Libohova, Pierre Roudier, Budiman Minasny, Hocine Bourennane

Hand-feel soil texture and particle-size distribution in Central France. Relationships and implications.

Anne C. Richer-de-Forges[1,7*], Dominique Arrouays[1], Songchao Chen[2], Mercedes Román Dobarco[3,4], Zamir Libohova[5], Pierre Roudier[6], Budiman Minasny[3,4], Hocine Bourennane[7]

1. INRAE, InfoSol Unit, 45075, Orléans, France
2. ZJU-Hangzhou Global Scientific and Technological Innovation Center, Hangzhou 311200, China
3. The University Sydney, School Life & Environmental Sciences, Eveleigh, NSW 2015, Australia
4. Sydney Institute of Agriculture, Eveleigh, NSW 2015, Australia
5. US Department of Agriculture-Agricultural Research Service, Dale Bumpers Small Farms Research Center, AR, USA
6. Manaaki Whenua -- Landcare Research, Private Bag 11052, Manawatū Mail Centre, Palmerston North 4442, New Zealand
7. INRAE, Unité de Science du Sol, 45075, Orléans, France

*Corresponding author: anne.richer-de-forges@inrae.fr

Highlights

Hand-feel soil texture and particle-size distribution are compared using a large database

The overall accuracy of hand-feel soil texture class allocation was 73%

Most discrepancies were explained by very fine and coarse sand content

Predicting soil water retention at pF2 using hand-feel texture gave satisfactory results

Abstract

Due to cost constraints, field texture classes estimated by hand-feel by soil surveyors are more abundant than laboratory measurements of particle-size distribution. Thus, there is a considerable potential to use field-estimated soil textures for mapping on the condition that they are reliable and can be characterized by a probability distribution function similar to values obtained by laboratory measurements. This study aimed to investigate and elucidate the differences between the field texture classes estimated by hand-feel and soil texture determined from particle-size analysis under laboratory conditions in a region of Central France. We tested several hypotheses to explain the discrepancies between field estimates and laboratory measurements (organic C content, pH, more detailed particle-size analyses, and CEC). Finally, we simulated the consequences of using particle-size distribution estimated from field texture on a pedotransfer function (PTF) for water retention. Laboratory measurements of clay, silt, and sand content for each field texture class were available for about 17,400 samples. Considering laboratory measurements and the French texture triangle as the reference, the overall accuracy of field texture class allocation was 73%, which was better than most of the results previously reported in the literature. When looking at each field texture class, most predictions were consistent; however, there were noticeable differences between a few field texture classes and particle-size classes. The extreme texture classes located at the corners of the texture triangle were better predicted than those located at the centre of the triangle. We found the discrepancy of field texture classes can be explained by the very fine sand (50-100 µm) and very coarse sand (1000-2000 µm) contents. Based on the particle-size distribution from each field texture class, we calculated their joint probability distribution function of their corresponding laboratory measurements of clay, silt, and sand content. Results showed that PTF values predicted using hand-feel texture were consistent with those obtained with the measured particle-size distribution. Overall, we demonstrated the value of hand-feel texture in expanding the soil texture database and supporting the expansion of the national database to inform soil water retention properties.

Keywords

Soil field texture; hand-feel test; particle-size distribution; texture classes; pedotransfer function

1. Introduction

Soil texture (ST) is the relative proportion of sand, silt, and clay in the soil. It is one of the most frequently measured soil properties. It can be either measured in the laboratory or estimated by soil surveyors in the field (NRCS-USDA, 2012). Soil texture influences a wide variety of soil properties, functions and behaviors, and a large range of pedological, physical, chemical, and biological processes in soil. It is a major controlling factor of important soil properties, such as hydraulic properties and water-holding capacity (e.g., Briggs and Lane, 1907; Veihmeyer and Hendrickson, 1927; Salter et al., 1966, 1969; Hall et al., 1977; Gupta and Larson, 1979; Bouma, 1989; Rawls et al., 1991; Pachepsky and Rawls, 1999; Arya et al., 1999; Wösten et al., 1999; Minasny and McBratney, 2002; Van Looy et al., 2017; Román Dobarco et al., 2019a, 2019b; Rudiyanto et al., 2021). This has led to an exponential increase of works on pedotransfer functions (PTFs). Many PTFs aim to predict hydraulic soil properties, especially soil water retention. Most PTFs use soil texture to predict soil properties that are either difficult or expensive to measure (Wösten et al., 2001; McBratney et al., 2002; Van Looy et al., 2017). In addition, ST is required in many dynamic simulation models (Ma et al., 2019).

There is also strong evidence that ST is one of the major controlling factors of soil organic carbon storage and sequestration potential, especially in temperate soils (e.g., Burke et al., 1989; Davidson and Lefebvre, 1993; Hassink, 1994, 1997; Arrouays et al., 1995; 2006; Chen et al., 2019). Finally, ST and its variations with depth are one of the main criteria used for soil class identification, both in international (e.g., Universal Soil Classification System: Hughes et al., 2017; Michéli et al., 2016; Soil Taxonomy: USDA-NRCS, 2014; World Reference Base for Soil Resources: IUSS Working Group WRB, 2015) and national classifications (e.g., Australia: McDonald et al., 1998; Isbell, 2016; Brazil: dos Santos et al., 2018; China: CRGCST, 2001; France: AFES, 2008; Germany: Blume et al., 2014; New Zealand: Hewitt, 2010; Russian Federation: Shishov et al., 2004).

Except for extreme events, such as severe erosion and deposition, or extensive flooding and alluvial deposits, ST is considered a relatively stable property, slowly evolving at the rate of weathering and pedogenic processes. Compared to soil properties that are more dynamic, the relative stability of ST is a considerable advantage, as more legacy data is being rescued and used to populate soil information systems (Arrouays et al., 2017). There are, however, severe limitations for combining ST estimates using different ST classification systems in a common database. First, the threshold values of particle sizes for determining texture classes are far from homogeneous between international and national classifications (e.g., International Society of Soil Science, 1929; Rousseva, 1997; Minasny and McBratney, 2001; USDA-NRCS, 2012; IUSS Working Group WRB, 2015). The use of different threshold values has led to the development of multiple continuous functions to transform particle-size distribution from one system to another (e.g., Shirazi and Boersma, 1984; Shirazi et al., 1988; Yaalon, 1989; Buchan, 1989a, 1989b; Rousseva, 1997; Nemes et al., 1999; Minasny et al., 2007; Takahashi et al., 2020). Second, soils are often classified according to ST classes, each having a given range of sand, silt and clay. These classes are generally drawn on triangular diagrams. These circumstances lead to further discrepancies between classifications as the class limits/intervals may largely differ between classification systems. Richer-de-Forges et al. (2008) illustrated this with a collection of textural triangles from the world. Most of the triangles are in good agreement on extreme classes (classes where the dominant particle-size fraction is either clay, silt, or sand). However, most of the discrepancies occur around the centre of the triangle, composed of ternary mixtures. The harmonization of ST classes and classifications worldwide is challenging because most texture triangles were developed or adapted to a regional pedological context. In the case of Australia, the hand-feel texture classes do not always correspond to the texture triangle classes (Minasny et al., 2007).

The standard laboratory analysis of sand, silt, and clay content (referred to hereafter as LAST, for Laboratory Analysis of Soil Texture) involves the dispersion of mineral particles after oxidizing the organic matter. The size classes for sand are separated using sieves and the silt and clay classes by sedimentation. This method used in this study is also known as the pipette method (AFNOR, 2003, NF X 31–107). Other existing methods (e.g. hydrometer method (Ashword et al., 2001), laser diffraction method (Ryżak and Bieganowski, 2011) were not used in this study. The field method to estimate ST through the hand-feel (hand-feel soil texture, referred hereafter as HFST) is based on a soil molded between fingers and thumb and is widely used by agricultural advisers and soil surveyors. Many studies (e.g., Vos et al., 2016; Salley et al., 2018) assessed whether both LAST and HFST yield the same ST classes, showing that a wide range of texture classes can be correctly assigned by soil surveyors (with overall accuracies ranging from more than 66% to 28%). Though these differences can be attributed in part to the different number of classes among the studies, and in some cases to the rather low number of samples, such a wide range remains questionable. These results suggest that the overall accuracy of predicting LAST using HFST determined by skilled soil scientists can hardly be generalized as it may depend on the pedological context and experience of the soil surveyors.

Less work has been conducted to derive laboratory-measured particle-size distributions from HFST classes. A comprehensive study on the performance of using HFST classes to predict soil particle-size distribution was conducted in Germany by Vos et al. (2016). It suggested that for a wide range of applications, the accuracy of HFST is sufficient and more time- and cost-effective than using LAST. More recently, in Australia, Malone and Searle (2021a) developed an algorithm that can generate plausible LAST profiles informed by the HFST class means. The simulations were done by sampling from the empirical distribution of LAST fraction data that characterised each HFST class. Malone and Searle then described how the HFST can be used to generate LAST fractions estimates with uncertainties to populate the Australian soil database. The idea of converting HFST classes to LAST values was also tested in the U.S. by Levi (2017).

Overall, there are several good reasons to explore the possibility of using HFST classes to derive proxies of particle-size distributions: i) numerous existing maps predict ST classes; ii) some PTFs are based on ST classes (e.g., Bouma, 1989; Wösten et al., 1995; Bruand et al., 2006; Al Majou et al., 2007, Piedallu et al., 2011); iii) as suggested by Vos et al. (2016), costs could be drastically reduced when using HFST instead of LAST; iv) field HFST class data are generally much more numerous than LAST in soil databases; and therefore (v) they could be used to improve the accuracy of particle-size predictions in soil mapping as demonstrated by Malone and Searle (2021b).

Though HFST data are much more numerous than LAST, they are inherently less accurate than LAST. The assessment of uncertainty coming from using different data sources is a topic that is constantly studied in digital soil mapping (DSM), as pointed out by Robinson et al. (2015). Recent review articles (Arrouays et al., 2020; Kidd et al., 2020; Searle et al., 2021) highlight the importance of providing uncertainties not only for the DSM products, but more importantly, to quantify how uncertainties from PTFs propagate when incorporated into models to derive final products for end-users (Amirian-Chakan et al., 2019; Libohova et al., 2019).

We hypothesize that the relations between HFST classes and LAST are not universal but closely linked with the pedological context. Therefore, we think that it is important to test these relations in new regions. In this study, we focused on the French Region Centre-Val de Loire, where a large number of soil data and other analyses could explain differences in HFST and LAST. Our objectives were:

1. To assess the overall accuracy of predicting HFST classes.
2. To explain discrepancies between HFST and LAST classes using pedological knowledge.
3. To model the distribution of LAST fractions for HFST classes.
4. To evaluate the uncertainty generated when using HFST classes to predict LAST and its consequences on a PTF for predicting soil water retention.

2. Material and methods

2.1. Study area

The study area is the French Region Centre-Val de Loire (Figure 1), which covers 34,151 km^2 and occupies the Middle Loire basin. The relatively flat topography (0–500 m) is traversed by the Loire River and several tributaries characterized by stepped-terrace systems mostly formed by processes of glacial–interglacial cycles. The alluvial formations show differences due to the influence of the lithology and tectonic processes (Voinchet et al., 2010). The climate is continental oceanic with an average annual temperature of 11.4 °C and mean annual precipitation below 800 mm (Joly et al., 2010). The economy of Region Centre relies strongly on agriculture, dominated by the production of cereal, oleaginous, and protein crops (about 70% of agricultural area). Other land uses include forests, pastures for bovine and caprine livestock, vineyards, and orchards. The main soil types according to the World Reference Base for Soil Resources (IUSS Working Group WRB, 2015) are Luvisols (ca 40%), Cambisols (ca 15%), Leptosols (ca 12%), Fluvisols (ca 11%), Podzols (ca 11%) and Planosols (ca 10%).

< Insert Figure 1>

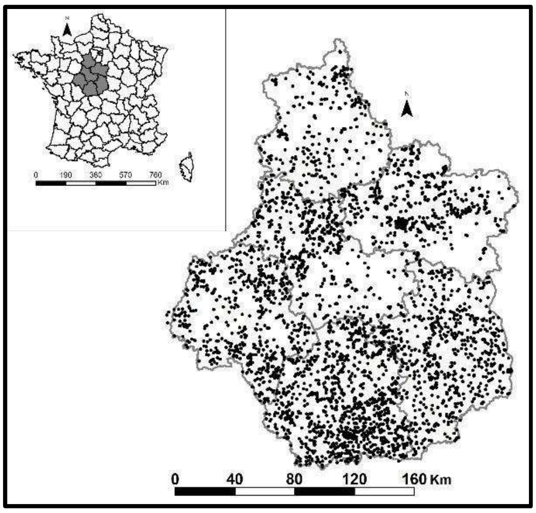

Figure 1. Location of Region Centre (France) and soil profiles for which soil texture was determined for horizons both in the laboratory and estimated in situ *by hand-feel.*

2.2. Soil data

A ST dataset was assembled from legacy profiles described and sampled during the main French national and regional soil mapping programs at 1:250,000, 1:100,000 and 1:50,000 scales. Thus, some clusters of profiles correspond to larger scale soil maps (Figure 1). A total of 3,862 soil profiles were stored in the database, including 17,388 soil horizons having both HFST and LAST measurements. About 150 experienced soil surveyors took part in the survey. The survey was mainly conducted at the department level (there are 6 departments in the region), or for small natural regions (SNR, there are 79 SNR in the region) by local soil surveyors who were experienced and highly skilled in identifying and describing soils in their natural environment.

For each horizon, HFST class was determined according to standard procedures (see Thien, 1979, and Ritchey et al., 2015) and recorded. The particle-size fractions used were clay (0-2 µm), silt (2-50 µm), and sand (50-2000 µm). The ST triangle used (Figure 2) was the equilateral “Aisne” triangle, which comprises 15 classes (Jamagne, 1967).

<Insert Figure 2>

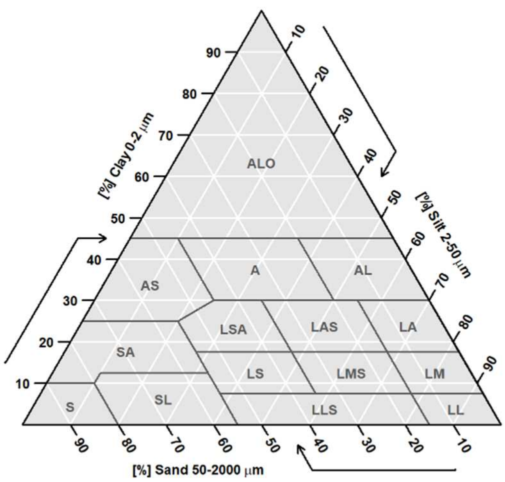

Figure 2. The soil texture triangle used in this study (from Jamagne, 1967) and tentative translation class name in English); ALO: heavy clay, A: clay, AL: silty clay, AS: sandy clay, LA: clayey silt, LAS: sandy clayey silt, LSA: clayey sand silt, SA: clayey sand, S: sand, SL: silty sand, LL: silt, LS: sandy silt, LMS: sandy medium silt, LM: medium silt, LLS: sandy silt.

Samples were air-dried, then gently crushed, and passed through a 2-mm sieve. Particle-size distribution was measured according to the pipette method, which is the French standard (AFNOR, 2003). Most of the original particle-size fractionations were determined based on either 5 (0-2, 2-20, 20-50, 50-200, 200-2000 µm) or 8 classes (0-2, 2-20, 20-50, 50-100, 100-200, 20-500, 500-1000, 1000-2000 µm). Particle-size fractions were grouped for clay (0-2 µm), silt (2-50 µm), and sand (50-2000 µm), but the original data was maintained for comparing HFST and LAST. Depending on the samples, other measurements may have included soil organic content (SOC) by dry or wet combustion, pH in a 1:5 soil-water ratio, and cation-exchange capacity (CEC) by the Metson method (AFNOR, 1999), as well as some more detailed particle-size fractions (see above). Topsoil (mainly ploughed and/or A horizons) and subsoil horizons were identified by a separate code.

2.3. Data Processing

2.3.1. Removal of Outliers

The sum of clay, silt, and sand and their relative percentage determined by LAST were calculated to check for ST data consistencies. When this sum was smaller than 90%, or larger than 110%, the LAST analyses were removed, whereas when the sum was between 90 and 110%, they were standardised to sum to 100%. Due to the large databases, a few errors may remain in both HFST and LAST data. Moreover, pure silt and clay ST do not exist in soils of this region. It is also unlikely that experienced soil surveyors will obtain some extreme discrepancies between their estimates. Therefore, we extracted for each HFST class its LAST particle-size distribution. For each HFST we considered as outliers all the values of sand, clay, and silt belonging to quantiles 0-0.5 and 99.5-100% of their LAST analyses. We made an exception for the sand LAST ST class for its clay content because some sandy soils do not contain any clay. We did not apply any other rules for removing outliers.

2.3.2. Confusion matrix and accuracy assessment

We built a confusion matrix to calculate different accuracies of the HFST classes by taking LAST classes as reference (Congalton and Green, 2008) and comparing them with accuracies reported from previous studies (e.g., Foss et al., 1975; Hodgson et al., 1976; Akamigbo, 1984; Post et al., 1986; David, 1999; Carlile et al., 2001; Minasny and McBratney, 2001; Franzmeier and Owens, 2008; Vos et al., 2016; Salley et al., 2018; Malone and Searle, 2021a). Following Rossiter (2004) and Salley et al. (2018), we calculated the accuracies described below:

- Overall accuracy (OA) represents the proportion of HFST classes that match LAST ST classes.
- User's accuracy (UA) assesses the proportion of HFST classes that match a given LAST class relative to the total number of estimated points of that HFST class (error of commission).
- Producer's reliability (PR) is a measure of the proportion of LAST ST classes correctly classified by the producer relative to the total number of observed points within each LAST ST class (error of omission).

These three indices were calculated as follows:

$$OA = \frac{\sum_{i=1}^{r} E_{ii}}{N} \quad (1)$$

$$UA = \frac{X_{ii}}{\sum_{i=1}^{r} X_{ij}} \quad (2)$$

$$PR = \frac{X_{jj}}{\sum_{i=1}^{r} X_{ij}} \quad (3)$$

where r is the number of texture classes, E_{ii} is the sum of diagonal elements, N is the number of observations, X_{ii} is the diagonal value for each class in one row, X_{ij} is the sum of values in one row or column, and X_{jj} is the diagonal value for each class in one column. These three indices range from 0 (worst) to 100% (best).

- Kappa coefficient (K) was calculated to account for unbalanced sample class distribution and measures classification accuracy after accounting for the probability of chance agreement among all the texture classes (Cohen, 1960). The kappa index is calculated based on the number of texture classes, number of correctly classified samples, and the total number of classes as:

$$K = \frac{P_0 - P_e}{1 - P_e} \quad (4)$$

where P_0 is the proportion of correctly classified samples and P_e is the probability of random agreement. Kappa results can range from -1 to +1.

We also calculated the Tau indicator, which measures the improvement of the classification over a random chance (Ma and Redmond, 1995; Rossiter, 2004).

$$Tau = \frac{\theta_1 - \theta_2'}{1 - \theta_2'} \quad (5)$$

Where

$$\theta_1 = \sum_{i=1}^{r} P_{ii} \quad (6)$$

$$\theta_2' = \sum_{i=1}^{r} P_i * P_{+i} \quad (7)$$

Confusion matrix and accuracy analyses were completed using the caret (Kuhn, 2008) and the psych (Revelle, 2011) packages in R version 4.0.5 (R Core Team, 2021).

2.3.3. Analysing the differences between HFST and LAST

We plotted the measured LAST particle-size distributions of horizons belonging to each HFST class using the R Package ‘soiltexture’: Functions for Soil Texture Plot, Classification and Transformation. Version 1.5.1 (Moeys et al., 2018). We also included ancillary variables, which could potentially explain inconsistencies between the two methods (e.g., SOC, pH, CEC, estimated CEC of clay, fine sand content and coarse sand content, some ratios between LAST fractions (when available)), and horizon depth (topsoil *vs* subsoil). We chose these variables from results obtained in previous studies (e.g., Foss et al., 1975; Hodgson et al., 1976; Akamigbo, 1984; Post et al., 1986; David, 1999; Carlile et al., 2001; Franzmeier and Owens, 2008; Vos et al., 2016; Salley et al., 2018). For each HFST class, we calculated the statistical distribution of the sample particle-size distribution using the R package ggplot2 version 3.3.3 (Wickham, 2009). As all our distributions summed to 100%, we calculated the joint distribution of clay and sand only.

We estimated the cation-exchange capacity (CEC) of the clay fraction using established equations that have been applied to French soils (Baize, 1993) and Danish soils (Rehman et al., 2019; Krogh et al., 2000):

$$CEC = a + (b \times Clay) + (c \times SOC) \quad (8)$$

where CEC is in centimoles of charge per kilogram, and clay and SOC contents are in percent mass.

From equation (8) the CEC of clay (CEC_{clay}) can be calculated as:

$$CECclay = \frac{[CEC - a - (c \times SOC)]}{Clay} \quad (9)$$

To adapt these formulas to the pedological context for our study area, we calibrated these PTFs using our data, either using all points or using topsoil and subsoil separately, as proposed by Krogh et al. (2000).

For all data, we obtained:

$$CEC_{all} = 0.109 + (0.441 \times Clay\%) + (1.625 \times SOC\%) \quad (10)$$

(Adjusted R-squared = 0.68)

For topsoils:

$$CEC_{top} = -0.108 + (0.493 \times Clay\%) + (1.139 \times SOC\%) \quad (11)$$

(Adjusted R-squared = 0.78)

And for subsoils:

$$CEC_{sub} = 0.281 + (0.421 \times Clay\%) + (1.880 \times SOC\%) \quad (12)$$

(Adjusted R-squared = 0.63)

However, when calculating CEC_{clay} using these formulas, we can obtain inconsistent values for soils with low clay contents and for high SOC contents. These discrepancies are outlined in Baize (1993) and will be discussed in section 4.2.4.

2.3.4. Uncertainty from PTFs generated to predict LAST particle-size distributions using HFST

Using the LAST particle-size distributions, we calculated their joint distributions for each HFST class to derive quantiles of the LAST particle-size distributions and estimate their range corresponding to given quantiles or prediction intervals. These uncertainties can be propagated when they are used in PTFs.

We calibrated a PTF for estimating gravimetric soil water content ($g.g^{-1}$) at field capacity (pF = 2.0 = -10 kPa ($\theta_{2.0}$) for France, using clay and sand as predictor variables with data from the SOLHYDRO dataset (Bruand et al., 2004). Then, we assigned the LAST class for each observation (clay, sand and $\theta_{2.0}$). We replaced the laboratory clay and sand measurements with the simulated clay and sand from the corresponding HFST class. The function was fitted again to predict the measured $\theta_{2.0}$. This process was repeated 100 times. We assessed changes in the PTF coefficients and regression performance (R^2, root mean square error, mean error) when using these proxies.

3. Results

3.1. Summary statistics

Table 1 describes summary statistics for the LAST particle sizes used in this study.

<Insert Table 1>

Table 1. Summary statistics for the LAST particle sizes used in this study (Region Centre-Val de Loire, France)

stc	n	mean %	std %	median %	min %	max %	range %	skew	kurt	ste	1st de	1st qu	3rd qu	9th de
CLAY	17388	27.99	16.21	26.23	0.00	92.50	92.50	0.77	0.56	0.12	8.50	16.00	36.92	49.80

SILT	17388	36.28	20.40	34.60	0.22	89.30	89.08	0.21	-1.02	0.15	9.60	19.20	52.90	65.70
SAND	17388	35.74	26.16	29.99	1.00	98.8	97.80	0.58	-0.80	0.20	5.90	12.50	55.00	76.40

stc: soil texture class; n: number of samples; mean: mean value; std: standard deviation; median: median value; min: minimum value; max: maximum value; skew: skewness; kurt: kurtosis; ste: standard error; qu: quartile; de: decile.

Except for sand, the mean and median values of LAST were very similar. The LAST values covered a wide range. The clay and sand distributions were skewed, whereas the silt distribution was only moderately skewed. The kurtosis of silt indicated a very flat distribution. Indeed, silt particles are present in most French topsoils, but with a very smooth concentration gradient from north to south (Arrouays et al., 2011). Overall, the particle-size distributions were not normally distributed.

3.2. Distribution of the LAST particle-size analyses in the texture triangle

Figure 3 displays the distribution of the LAST particle-size analyses distribution in the ST triangle.

<Insert Figure 3>

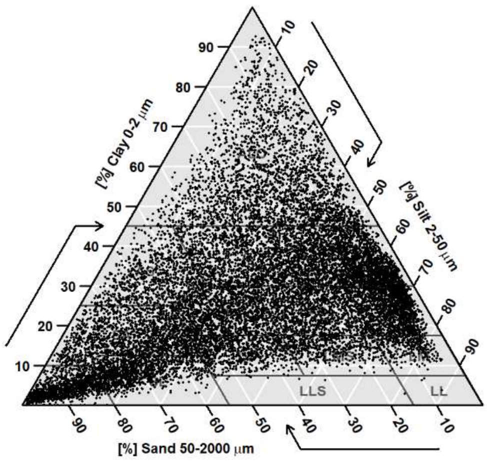

Figure 3. Distribution of the measured particle-size analyses used in this study in the French textural triangle diagram of Jamagne (1967).

Interestingly, this distribution is similar to those shown by Román Dobarco et al. (2016) using different databases covering topsoil (< 0.5 m depth) of all of mainland France. In particular, we noted a large number of missing values along the clay-sand and sand-silt axes, and in particular, the LLS (sandy medium silt) and LL (sandy silt) classes. This suggests that some clay-sand or sand-silt pure binary mixtures are rarely observed, partly due to particle-size sorting during erosion, water or aeolian transport of sediments. We also observed (as outlined in Table 1) that extreme values (equal to 0 or 100%) of all particle sizes are missing, except for the zero-clay value, which is due to the rule we applied for filtering the outliers on the sand class. Indeed, some pure sand horizons may exist in some alluvial areas. Overall, the distribution of particles in the ternary diagram suggested that the study area shows a diversity of particle-size distributions comparable to the diversity observed in the entire French mainland territory. We noted, however, that most silty fractions (especially medium silt) are less encountered in the Region Centre-Val de Loire, compared to entire France diagrams, which may be explained by the fact that the loess belt covers mainly the northern and western parts of France (Bertran et al., 2016).

3.3. Confusion matrix and accuracy assessment

Table 2 shows the confusion matrix between HFST classes (rows) and the LAST classes (columns).The bold numbers in the diagonal are the number of correctly identified observations.

Table 2. Confusion matrix between hand-feel predicted ST classes and their corresponding ST classes using measured particle-size distribution. Users' accuracy (UA, Eq. 1) and producers' reliability (PR, Eq. 3) for the ST classes are determined by hand-feel test and by laboratory measurement of particle-size distribution. The reference (or considered as "true") values are the values from laboratory measurement. ALO: heavy clay, A: clay, AL: silty clay, AS: sandy clay, LA: clayey silt, LAS: sandy clayey silt, LSA: clayey sand silt, SA: clayey sand, S: sand, SL: silty sand, LL: silt, LS: sandy silt, LMS: sandy medium silt, LM: medium silt, LLS: sandy silt.

<Insert Table 2>

ST hand-feel class	ST measured particle-size class															sum	UA%
	A	AL	ALO	AS	LA	LAS	LL	LLS	LM	LMS	LS	LSA	S	SA	SL		
A	**1195**	353	261	69	5	43	0	0	0	0	0	29	0	1	0	*1956*	*61*
AL	146	**1456**	93	3	68	22	0	0	0	0	0	10	0	0	0	*1798*	*81*
ALO	71	49	**2064**	21	0	0	0	0	0	0	0	0	0	0	0	*2205*	*94*
AS	123	5	39	**643**	0	2	0	0	0	0	2	60	0	73	3	*950*	*68*
LA	33	231	15	0	**1303**	128	0	0	6	3	3	53	0	0	0	*1775*	*73*
LAS	84	105	15	12	91	**877**	0	0	2	33	26	145	0	12	0	*1402*	*63*
LL	2	2	0	0	15	3	**3**	2	11	9	2	2	0	0	0	*51*	*6*
LLS	0	3	0	0	17	13	0	**3**	7	19	52	5	1	4	7	*131*	*2*
LM	8	29	0	0	164	36	0	0	**290**	42	21	8	0	0	0	*598*	*48*
LMS	8	12	0	1	42	91	0	0	30	**382**	129	27	0	19	2	*743*	*51*
LS	9	1	0	0	0	11	0	3	0	30	**444**	38	0	34	24	*594*	*75*
LSA	32	24	0	26	18	94	0	0	0	6	46	**836**	0	48	1	*1131*	*74*
S	0	0	0	5	0	0	0	0	0	0	10	6	**1151**	133	256	*1561*	*74*
SA	12	0	0	90	0	4	0	0	0	0	28	83	15	**1144**	64	*1440*	*79*
SL	0	0	0	0	0	7	0	2	0	8	52	13	43	93	**835**	*1053*	*79*
sum	*1723*	*2270*	*2487*	*870*	*1723*	*1331*	*3*	*10*	*346*	*532*	*815*	*1315*	*1210*	*1561*	*1192*	***17388***	
NA	108	190	188	78	245	171	1	7	92	92	77	75	91	91	77		
PR%	*69*	*64*	*83*	*74*	*76*	*66*	*100*	*30*	*84*	*72*	*54*	*64*	*95*	*73*	*70*		*OA%=73*

PR% is producer's reliability; UA% is user's accuracy; OA is percent correctly classified; NA is non available data for ST hand-feel class.

The overall accuracy was 73%. UA% (how well HFST corresponds to LAST) ranged from 2-94% while PR% (how well LAST relates to HFST) ranged from 30-100%. Note that UA% and PR% are often unreliable with smaller sample sizes and unbalanced class distribution (Congalton and Green, 2008). This is noticeably the case for the French HFST and LAST belonging to LL (silt) and LLS (sandy silt), for which very few samples are available (see also Figure 3). Also, the class distributions are very unbalanced. Kappa and Tau indices were 69.8% and 70.66%. This indicates that OA% only slightly overestimates the performances.

The graphic representation of the differences obtained for ST classes is presented in Figure 4.

<Insert Figure 4>

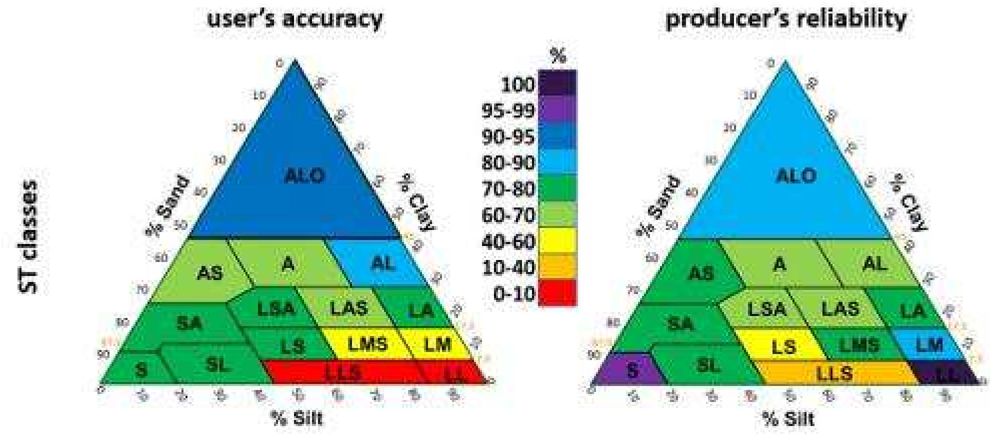

Figure 4. Users' accuracy (UA%) and producers' reliability (PR%) by soil texture (ST) class.

The UA% had a lower performance for most silty textures (considering the low and/or unbalanced number of samples in ST classes LL, LLS and LM - see Table 2). Note also that the PR% performances were almost larger than 60%, except for LS and LLS ST classes, which indicates that these classes are characterized by a larger dispersion of LAST ST values than the other ones. When looking at the PR% of extremely silty or sandy classes, the results were nearly perfect, indicating that there is no difficulty in identifying those samples having a very large proportion of sand or silt.

3.4. Possible causes of observed inconsistencies between the two ST classes

As explained in section 2.3.2, we plotted the LAST particle-size distributions of horizons belonging to each HFST class, separating topsoil from subsoil, and adding a color legend of some ancillary variables (when available), which could potentially explain inconsistencies between the two methods. We present here the main results. The first striking example is that we did not observe any obvious effect of SOC on ST misclassification.

3.4.1. Particle-size fractions

3.4.1.1. Sand fractions

When looking at the effect of very coarse sand (VCS: 500-2000 µm), the main misclassifications were observed for HFST classes A (clay) and AS (sandy clay) (Figure 5) for which very low VCS content

(<50 g kg^{-1}) led to shifts of LAST classes from A to AL (silty clay) or ALO (heavy clay) classes, and from AS to several classes, most often to the A (clay) class.

<Insert Figure 5>

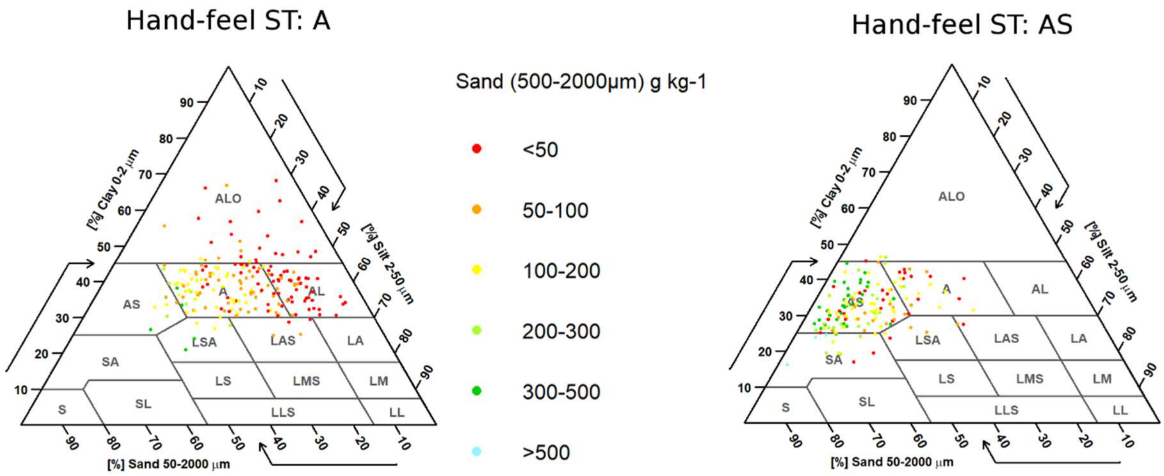

Figure 5. Effect of very coarse sand content (VCS) on HFST misclassification for subsoil A (clay) and AS (sandy clay) classes (subsoil). Projected points are from LAST analyses; point colors correspond to different classes of VCS content from LAST measurements, when available.

The most striking effect of coarse sand content (200-2000 µm) was observed for the subsoil HFST classes LMS (sandy medium silt) and LAS (sandy clayey silt) (Figure 6). A high coarse sand content often led to a lateral shift to their adjacent LAST classes richer in sand, whereas low coarse sand contents often led to underestimating LAST silt and/or clay content.

<Insert Figure 6>

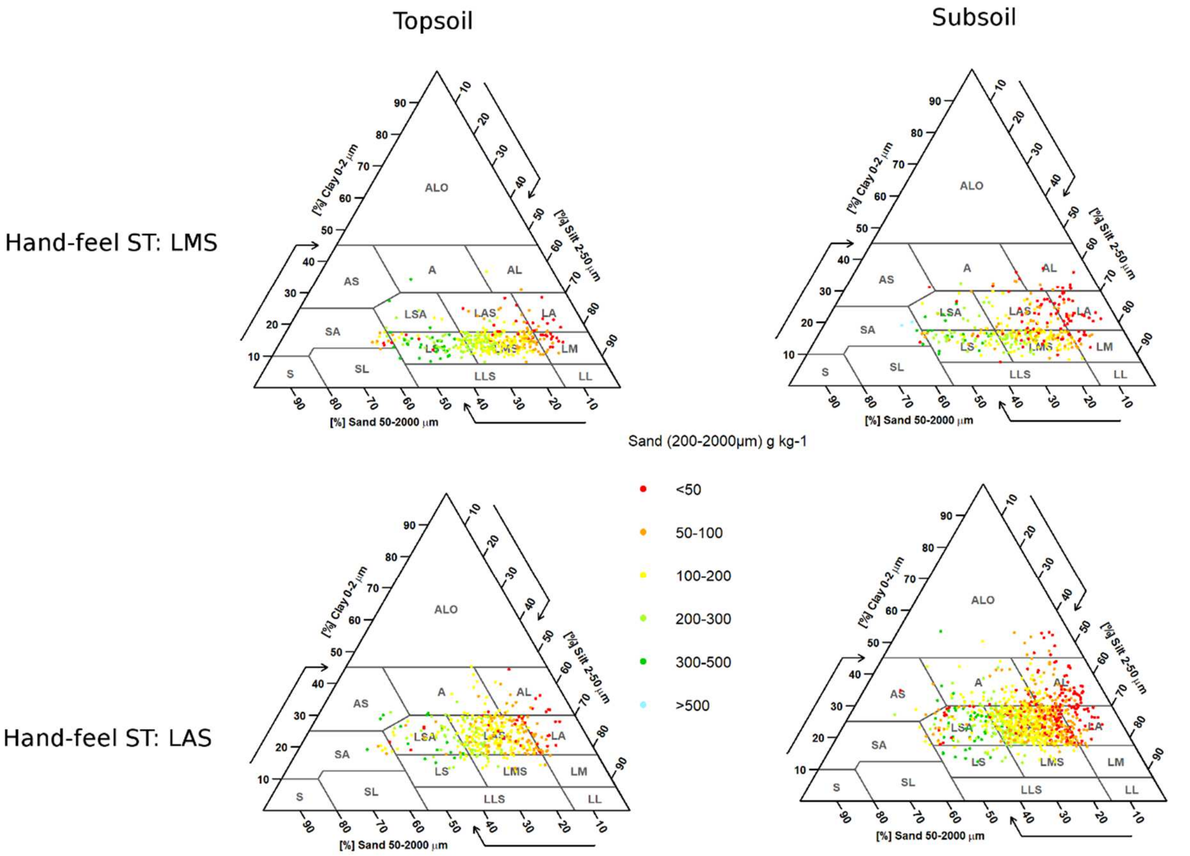

Figure 6. Effect of coarse sand content on HFST class misclassification for LMS (sandy medium silt) and LAS (sandy clayey silt) classes. Projected points are from LAST analyses; point colors correspond to different classes of coarse sand content from LAST measurements, when available.

The effect of very fine sand (VFS: 50-100 µm) was evident and presented a tactile confusion with silt fractions. Surveyors cannot differentiate low (< 50 g kg^{-1}) and large VFS content (> 200 g kg^{-1}). For example, HFST LM (medium silt) subsoil and LMS (sandy medium silt) topsoil were, in fact, more sandy/less silty LAST classes (Figure 7).

<insert Figure 7>

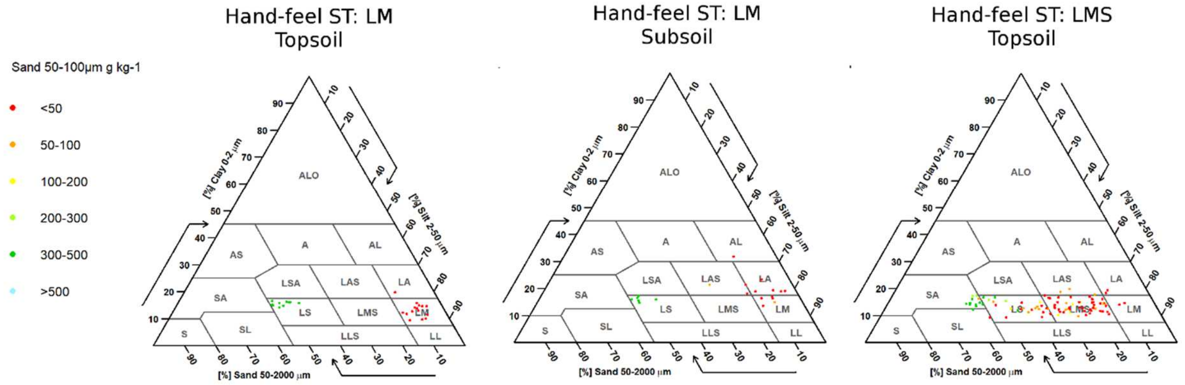

Figure 7. Effect of very fine sand content on HFST on LM (medium silt) and LMS (sandy medium silt) class misclassifications. Projected points are from LAST analyses; point colors correspond to different classes of very fine sand content from LAST measurements, when available.

For some HFST classes that were silty but more clay (both topsoil and subsoil for LA and LAS and topsoil for AL) we also observed a lateral shift towards more sandy/less silty LAST classes when the VFS content was large (Figure 8).

<insert Figure 8>

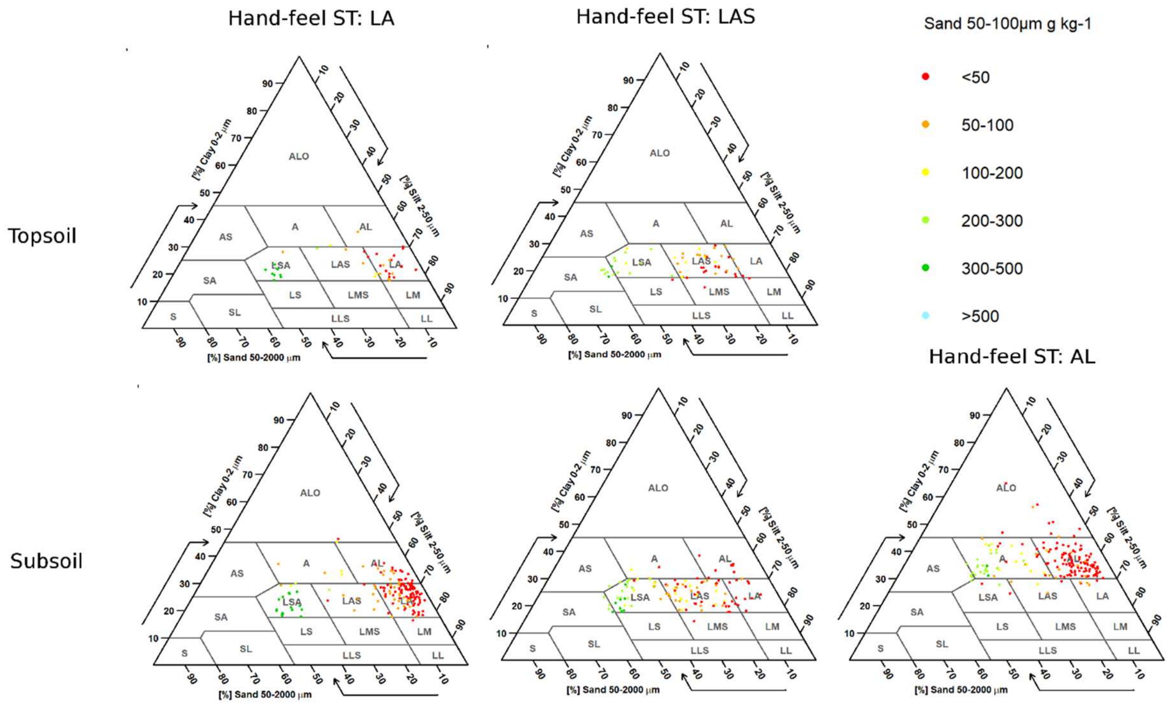

Figure 8. Effect of very fine sand content on HFST on LA (clayey silt), LAS (sandy clayey silt), and AL (silty clay) class misclassifications. Projected points are from LAST analyses; point colors correspond to different classes of very fine sand content from LAST measurements, when available.

Surprisingly, a small content of VFS seemed to lead to an underestimation of silt in the HFST class S (sand), (Figure 9). We found it to be a surprising result, because we expected that VFS could result in a similar hand-feeling as silt.

<insert Figure 9>

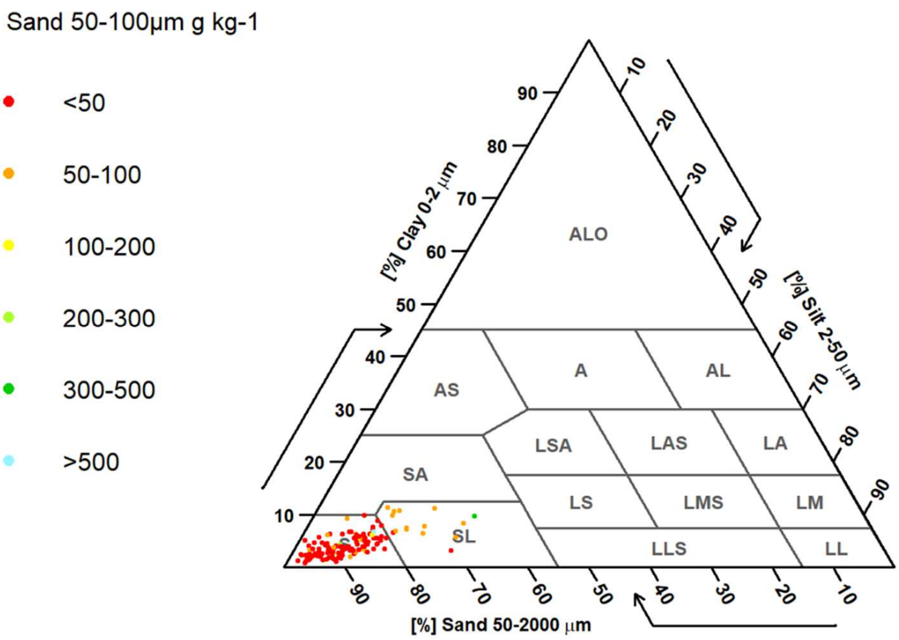

Figure 9. The unexpected effect of VFS fraction on the LAST particle-size distribution of the HFST sand (S) class for topsoil. Projected points are from LAST analyses; point colors correspond to different classes of very fine sand content from LAST measurements, when available.

3.4.1.2. Silt fractions

The analysis of the distribution of silt fractions did not provide any clear information except for the HFST LA (clayey silt) for which high values of the ratio fine silt (2-20 µm) to coarse silt (20-50 µm) were related to underestimations of LAST clay or sand content values (Figure 10).

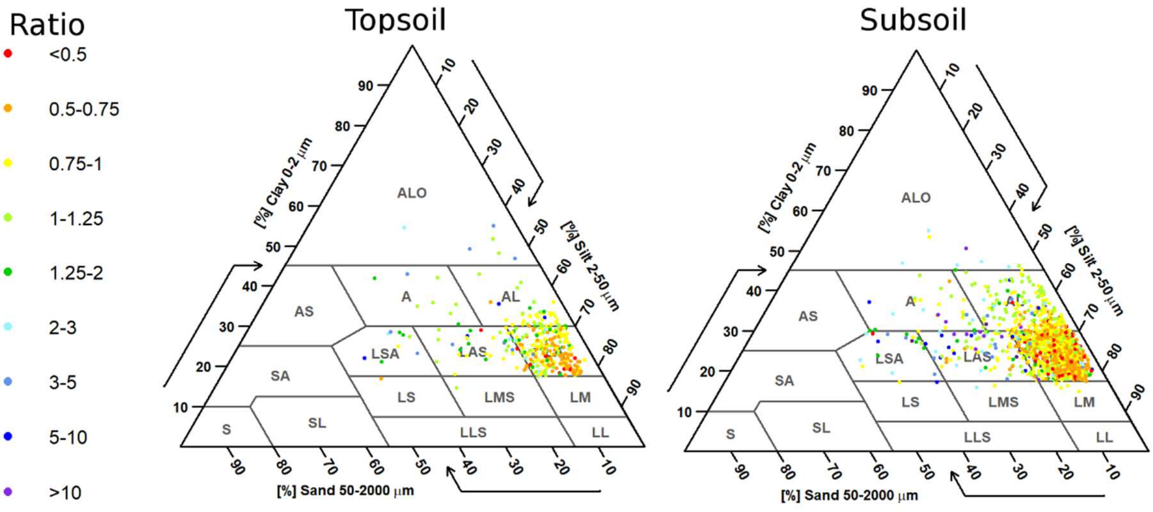

Figure 10. Relationships between the ratio fine silt (2-20 µm) to coarse silt (20-50 µm) fractions and the HFST class LA (clayey silt). Projected points are from LAST analyses; point colors correspond to different classes of ratios fine silt/coarse silt from LAST measurements, when available.

3.4.2. CEC and CEC_{clay}

3.4.2.1. CEC

The only noticeable result for CEC was a tendency to underestimate clay content for the HFST A (clay) (Figure 11). At first glance, this result seems counterintuitive. Possible explanations are discussed in section 4.2.4.

<Insert Figure 11>

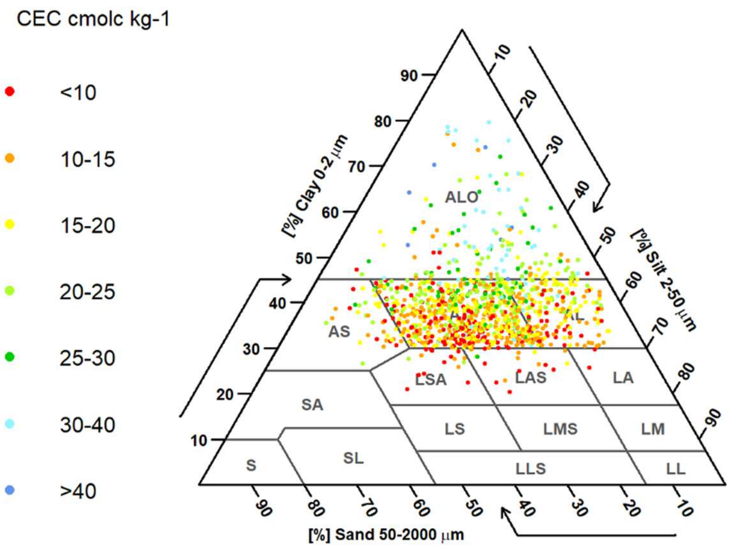

Figure 11. Relationships between CEC and misclassifications of the HFST A (clay) subsoil. Projected points are from LAST analyses; point colors correspond to different classes of CEC from LAST measurements, when available.

3.4.2.2 CEC_{clay}

The calculation of CEC_{clay} using equation 9 and applying the coefficients found in equations 10, 11, and 12 for all topsoil and subsoil samples, respectively, led to some inconsistent results, with some values highly negative and some highly positive. Moreover, even when we considered the negative and the highly positive values as outliers, we could not find any clear tendency, except for very high CEC_{clay} values in sandy soils (Figure 12).

<Insert Figure 12>

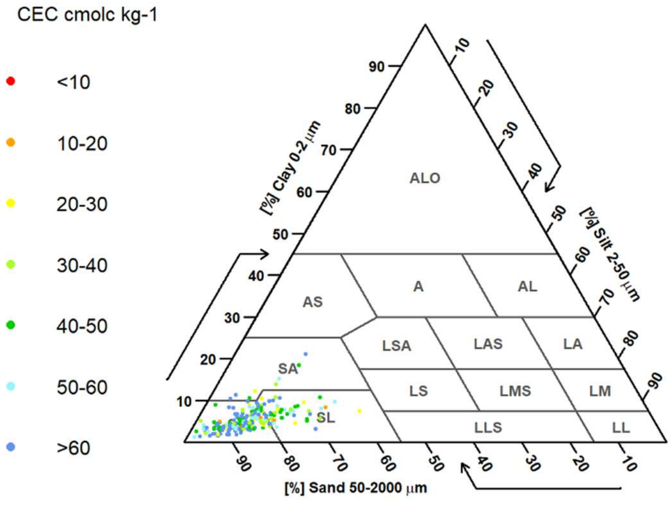

b

Figure 12. Unexpected very high CEC_{clay} values in S (sandy) topsoils. Projected points are from LAST analyses; point colors correspond to different classes of very find sand CEC_{clay} values calculated using equations 9 and 10 from LAST measurements, when available.

3.5. Joint distributions of the particle-size distribution of HFST classes and their effects on a PTF predicting water retention

We calculated the joint distribution of the measured particle-size distribution for each HFST class. As all our particle-size fractions sum to 100%, we plotted these distributions using only clay and sand as x and y axes, respectively (supplementary material S1). These results clearly showed that the shape and the extent of the distributions depend on the HFST classes, both according to their relative area in the triangle and to the accuracy of their classifications when compared to LAST particle-size distribution.

Using LAST data from a soil database, we obtained the following PTF for water content at field capacity for French soils:

$$WC_{2.0} = 0.171974 + (0.002259 \times Clay\%) + (-0.000998 \times Sand\%) \quad (13)$$

where $WC_{2.0}$ is the gravimetric soil water content (g g^{-1}) at pF 2.0, and Clay% and Sand% are in g $100g^{-1}$. The results of the 10-fold cross-validation repeated 10 times for this PTF had on average an R^2 = 0.599 and RMSE = 0.0437 g g^{-1}.

We then replaced the clay and sand data from the data that generated this PTF with their corresponding ST classes. The PTF was calibrated again but using simulated clay and sand from corresponding HFST classes. The process was repeated 100 times, and the resulting distribution of parameters of the PTF (Eq. 13) are shown in Figure 13. The distributions of clay, silt, and sand for the ST classes are described in supplementary material S1.

< Insert Figure 13>

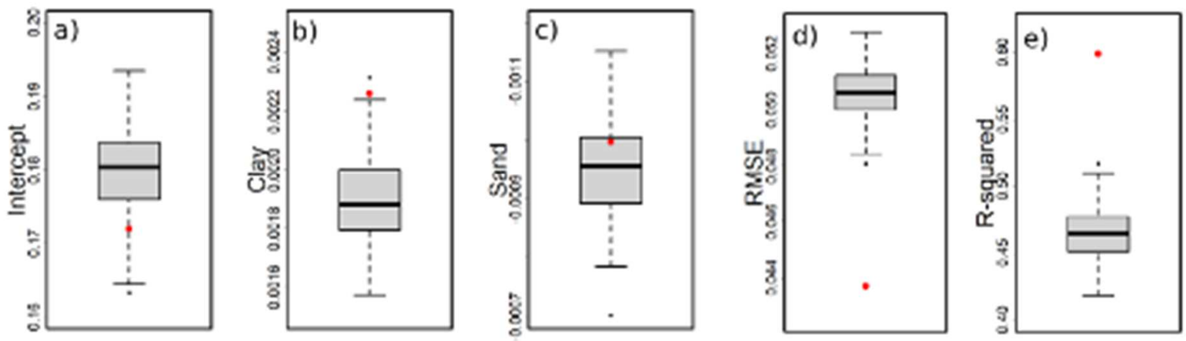

Figure 13. Box plots of the parameters of PTF predicting field capacity using 100 times random resampling from the distributions of soil texture described in supplementary material (S1). a) intercept; b) coefficient for clay content; c) coefficient for sand contents; d) Root Mean Square Error (RMSE); e) R-squared (R^2): coefficient of determination. Red points are the results of the cross-validation of the PTF predicting the gravimetric soil moisture at pF = 2, using measured clay% and sand% as predictors. The mean RMSE and R^2 were calculated with 10-fold cross-validation repeated 10 times.

The intercept of the PTF calculated using the LAST data is located outside the interquartile range of the intercepts obtained from the simulations. The box plot for clay coefficients estimated from HFST did not overlap with the clay coefficient using the LAST data, but its value remained very close. For sand, the coefficient obtained from LAST data fell within the interquartile range of the box plot. Note that the RMSE we obtained are larger but remain relatively comparable with the LAST data PTF.

Similarly, the R^2 obtained using the LAST data PTF in cross-validation decreased when using simulated clay and sand content from HFST.

4. Discussion

4.1. ST classes and performance indices

Rossiter (2004) stated that “a map with a few large classes may appear more accurate than one with many classes, simply because of the simpler legend”. Most soil texture triangles have between 12 and 18 classes, although they may also have simplified versions that groups some of the classes. The French triangle used in our study had an average and a median number of ST classes, similar to triangles used worldwide (Richer-de-Forges et al., 2008). However, there is a wide range in the number of texture classes sometimes due to the scale of mapping and the geomorphology characteristics of countries. For example, there are very simplified triangles with only 5 classes, such as the one used for the 1:1 000 000 scale map of E.U. (King et al., 1994) or the one from the Harmonized World Soil Database (version 1.0), with only 3 classes (FAO/IIASA/ISRIC/ISS-CAS/JRC, 2008). The first French triangle (Lagatu, 1905, no longer used) with only 7 classes is another example not used in our study. On the other side of the spectrum, there are very detailed triangles, such as the German one (Sponagel et al., 2005) with 37 classes and the Polish one with 23 classes (Polish soil classification, 1989). The Australian texture triangle (based on LAST) has only 11 classes, but the HFST contains up to 47 classes (Malone and Searle, 2021a). The most detailed soil texture triangles have often been drawn to capture the pedological/textural context of a region or country. For example, the Polish triangle has many detailed classes for low clay content sandy soils because of the country’s predominance of sandy and sandy clay soils (Kowalkowski et al., 1994). On the other hand, the German triangle has many small classes in the very sandy and silty textures due to the presence of both sandy soils and loess-derived soils (Kruse, 2016). In Australia, the HFST has 17 classes for describing clay texture due to the abundance of clay soils (Malone and Searle, 2021a).

Most of the studies about the HFST determined by well trained professional soil scientists (e.g., Foss et al., 1975; Hodgson et al., 1976; Post et al., 1986; Akamigbo, 1984; Levine et al., 1989; Ogunkunle, 1993; David, 1999; Rawls and Pachepsky, 2002; Pachepsky et al., 2006; Salley et al., 2018) showed a wide range of OA% (from more than 66% to 28%). Even if some of these differences can be attributed in part to the different number of classes among the studies, and in some cases to the rather low number of samples, the OA% observed in our study (73%) suggests that the performance in central France was among the best ones, especially given the wide range of LAST that were tested (see Figure 3). This finding is also corroborated by the Kappa and Tau values that were very close to OA%. However, these excellent results need to be considered in the context. The HFST observations were made by experienced soil scientists with a good knowledge of the pedological conditions of their region. Also, there were many collaborations at the borders of the "départements" and a strong regional coordination (Richer-de-Forges et al., 2014). Nevertheless, the observations from this study could vary widely and should not be generalized to other parts of the country or the world.

In the literature, the precision of HFST varied for different ST classes, but there was no consistent finding. Some studies showed that extreme classes were better predicted, while others suggested that the central classes were better estimated. Salley et al. (2018) argued that the dominance of one size fraction within a class facilitates accurate estimates of the sand and heavy clay HFST classes because they are easier to be estimated in the field. They attributed the relatively poor results for classes with more silt content because of inexperienced surveyors and the fact that soils with high silt were less abundant in the region. However, this is not the case in central France, except for LL and LLS classes for both HFST and LAST, which are less abundant in this region. The low number of LL and LLS ST samples means that our results need to be interpreted cautiously. Nevertheless, the PR% of extreme soil classes is higher than those of the central classes, which confirmed that experienced soil scientists could identify extreme ST classes. Our results are also consistent with the findings of Rawls and Pachepsky (2002) who showed that with the USDA textural classes, loamy textures located in the centre of the triangle were among the HFST classes having the least agreement with LAST classes. Vos et al. (2016), however, concluded that whenever one major soil texture fraction (sand, silt, clay) dominates, the content of this texture fraction is underestimated by the field texture. They postulated that the scarcity of data points in the absolute extreme regions of the ST triangle could have been one of the reasons.

When comparing OA%, UA% and PR% we should also keep in mind that the areas covered by ST classes in the triangle (and thus, the range of particle-size values) differ among ST classes. Using the USDA 12 ST classes triangle, Foss et al. (1975) attributed the largest accuracy of some HFST classes to the larger portion of the textural triangle taken up by these classes. This is also why Vos et al. (2016) obtained rather low accuracies using the German texture triangle, because many classes occupy a small area in the triangle, especially for the range of particle size of their samples.

4.2. Sources of discrepancies between HFST and LAST

In this section, we discuss some of the potential main sources of discrepancies between HFST and LAST. We first examine differences due to methods and then the influence of other soil properties.

4.2.1. Inherent differences and sources of errors between the methods

By definition, HFST is mainly a tactile test based on the mechanical behaviour of the soil. Briefly, and according to practical guidelines such as those from Thien (1979) and Ritchey et al. (2015), sand feels gritty to the touch and holds very little water when the soil is rather dry, whereas dry silt particles feel like flour or baby powder. When wet, silt feels smooth and muddy. Clay feels sticky when wet and hard and brittle when dry. These tactile feelings can be aided by visual or audio examinations (for example, to detect very fine sands) or other tests such as Thien (1979). HFST is subjective, and its accuracy is highly constrained by the operator's experience and their local knowledge of the pedological and mineralogical context. Moreover, this tactile HFST is performed on the whole soil, so that the HFST results can be influenced by other soil characteristics such as organic matter.

LAST is less subjective, as it is measured using standard procedures. However, LAST is based on Stokes' law (Stokes, 1851), assuming the particles are spherical, which is often not the case. Baize (1993) stated that the coarse silt (20-50 µm) particle-size fractions might exhibit more errors than other ones because they are often calculated by the difference between the sand and the 0-to-20 µm fractions. Moreover, LAST is not based on the same type of mechanical behaviour as HFST; LAST is mainly based on grain sizes sorted by sieving sands, and by sedimentation process for finer particles, whereas HFST is a mechanical test that is more comparable to Atterberg's tests (Atterberg, 1905). Therefore, one can understand that depending on the pedological context (e.g., soil parent material, conditions of sedimentation (Chrétien, 1971), weathering and pedogenesis (Robert et al., 1991; Hardy, 1993), clay mineralogy and the presence of non-clay particles in the finest fractions (Hardy, 1992; Hardy et al., 1999), and the shape of coarser particles (Chrétien, 1971; Chrétien and Bisdom, 1983)), similar LAST classes can exhibit different behaviors and thus can lead to different HFST classes. Factors such as gypsum and iron can also lead to considerable discrepancies between HFST and LAST. With gypsum, it is mainly related to dispersion. With iron, it is due to microaggregation. There are however, very few soils containing gypsum in central France, and microaggregation due to iron is known to mainly occur in tropical and sub-tropical soils.

4.2.2. Influence of SOC and pH

Although there are some well-known relationships between pH_{water} and ST, because of the effect of clay on soil's pH buffering capacity, and well-known relationships between ST and SOC content (previously evidenced in France by Arrouays et al., 2006), we could not prove any influence of those factors on the misclassification of HFST classes when compared to LAST classes. This is not surprising for pH_{water}, although it has been shown that pH can influence clay's rheological properties (Gori, 1994). However, we expected some effects of SOC content. Indeed, as pointed out by Salley et al. (2018), soil samples with high SOC content may "impart a greasy silty feel, reducing coherence of clay and causing an underestimation of clay". This was observed and discussed by several authors (e.g., Foss et al., 1975; Hodgson et al., 1976; Vos et al., 2016; Salley et al., 2018). The “silty feel” of SOC might also induce overestimates of silt fractions by HFST, especially in sandy, loamy, and silty soils (Foss et al., 1975). Our results do not indicate such an effect, despite topsoil SOC content reaching 14.6 %. Most of the sandy soils from our study are mainly composed of coarse and very coarse sand (data not shown), thus the “gritty” feel may have overcome the effect of SOC. In addition, our study excluded O horizons, and thus very high SOC contents were nearly absent.

4.2.3. Influence of the distribution of particle-size fractions

Our results indicated that the finer particle-size fractions provide new insights on their effect on HFST misclassifications. Although never clearly demonstrated in the literature, the effect of VCS on the misclassifications for HFST classes A and AS is logical. Very low values of VCS make the soil feel less gritty and often lead to an underestimation of silt or clay. The striking example of the effect of total coarse sand content on the misclassification of subsoil HFST classes LMS and LAS is reasonable. High coarse sand contents often lead to a lateral shift to their adjacent LAST classes richer in sand, whereas low coarse sand contents often lead to an underestimation of LAST silt and/or clay content.

The clear effects of VFS content are mostly attributed to the tactile confusion of silt fractions with VFS fractions. The counterintuitive effect of VFS on HFST sand class misclassification may be linked to the fact that coarse silt and VSF contents are often related as they are very narrow adjacent soil particle-size classes, which can also result from the same sedimentation or pedogenic processes. Here we assume that LAST is the more accurate standard, but the procedure for determining the VFS content depends on sieving, which may be subject to error.

Finally, for the HFST class LA, high values of fine silt (2-20 µm) to coarse silt (20-50 µm) ratio were related to the underestimation of clay or sand content. This is more difficult to explain, unless we take into account that in this region, most of the LAST LA soil textures are located in soils derived from rather homogeneous loess deposits (Chen et al., 2021). In this case, the soil surveyor's experience and knowledge and their landscape analysis are essential in helping them assign the right

ST class to these horizons. In other words, the HFST determination sometimes benefits from other indicators, such as color, lithology, and landscape position (McDonald et al., 1998; Rawls and Pachepsky, 2002; Salley et al., 2018). This underlines the fact that the experience of the soil surveyor in a given pedological context is one of the prerequisites for good accuracy of LAST predictions based on HFST (e.g., Akamigbo, 1984; Franzmeir and Owens, 2008; Levine et al., 1989; McDonald et al., 1998; David, 1999; Salley et al., 2018). Therefore, although there is a great potential for citizen soil science to assist digital soil mapping (Rossiter et al., 2015) it is unlikely that untrained citizens would be able to bring reliable information on ST, except for the extreme texture classes.

4.2.4. Influence of CEC and CEC_{clay}

CEC did not have a strong influence on HFST classification accuracy. There was an underestimation of clay content of the HFST class A for the highest CECs. This could have been due to higher SOC contents in the samples with higher clay, but this was not confirmed by the results of our study (see section 3.4.). Salley et al. (2018) indicated that some very clayey soils may form micro-aggregates that are difficult to break down by hand because of their high degree of stability. Similarly, Searle and Malone (2021a) observed that for the same HFST class, there was a higher clay content in the so-called sub-plastic soils compared to non-sub-plastic soils. This sub-plasticity could be due to the microaggregation described above.

There was no relationship between CEC_{clay} and misclassification of texture classes. We expected that clay mineralogy and/or the presence of non-clay particles in the finest fractions (Hardy, 1992; Hardy et al., 1999) would have an effect on misclassification. Indeed, simple clay percentage does not capture variation in mineral composition. As stated by Salley et al. (2018) and McDonald et al. (1998), we cannot exclude the fact that errors because of clay mineralogy may be reduced through calibration with locally sourced soils, where mineralogy is relatively uniform, and supplemented by additional indicators of mineralogy (e.g., those based on color or landscape position). Therefore, the experience and local knowledge of the soil surveyor may have played a major role in the lack of relationship between CEC_{clay} and misclassification. However, we should consider that our prediction of CEC_{clay} is probably inaccurate, as evidenced by some of the aberrant values. The surprising observation of very high CEC_{clay} values in the sand HFST class topsoil could be due to an overestimation of the CEC of SOC in this class. Indeed, SOM is often composed of unbound and particulate SOM in sandy soils, which generally has a lower CEC than more stable SOM. This assumption is consistent with the large difference in C:N ratio in sandy soils compared to other soils (Figure 14).

<insert figure 14>

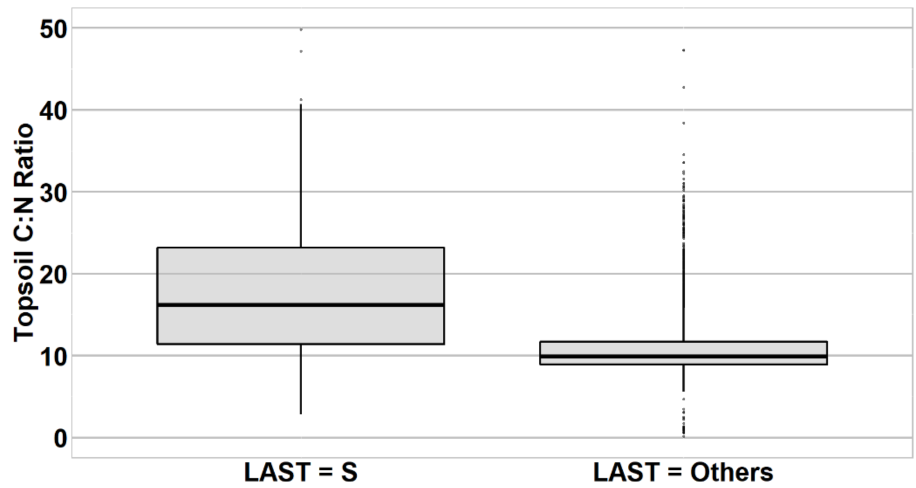

Figure 14. Box plots of C:N ratio of topsoil being classified as sand by LAST analyses (left) and the other LAST ST classes (right).

In summary, our estimates of CEC_{clay} probably have many sources of error. We tried various other available variables to see if they were related to the distribution of residuals, but we did not find any trends. Further studies are needed to evaluate whether better equations could predict CEC and CEC_{clay} based on the data used in our study.

4.3. The impact on a pedotransfer function

The pedotransfer function calibrated from the HFST simulations was reasonably consistent with the one obtained with LAST. Even if the values of the PTF coefficients differed slightly, we should keep in mind that their absolute values were very close. Thus, the coefficients will not have a large impact on the predicted values of water content at field capacity. This is confirmed by the comparable RMSE and R^2 values. More generally, the discrepancies in R^2 and RMSE may be due to two reasons: 1) there was an incorporation of error due to resampling from the joint distribution, and 2) the joint distributions of particle-size fractions for each ST class came from a different sample than the calibration dataset for the PTF (SOLHYDRO). Specifically, our resampling sometimes led to the selection of some values that were out of the calibration domain of the PTF, even for the particle-size distribution. As noted in section 3.2., the range of values that were covered by the sampling in the Region Centre-Val de Loire is larger than the range covered by SOLHYDRO (Bruand et al., 2004; Al Majou et al., 2007), especially for the values close to the clay-sand and sand-silt borders of the ST triangle. Whereas most ST classes were well represented in the dataset from Region Centre-Val de Loire, it is possible that the joint distributions for each HFST class differ somewhat from the empirical joint distributions for each ST class in the calibration dataset. This leads to two issues to consider:

i) The region in our study is not necessarily representative of all French soils, as previously shown by Chen et al. (2018) when mapping the validity domain of a completely different PTF, aiming at predicting bulk density.

ii) One drawback of this method is that we implicitly assumed that the soil surveyors would have correctly assigned the particle-size distributions of the original data to the right ST class by feel. Nevertheless, we can confirm the accuracy of HFST by the very good results obtained for the OA, UA and PR% (see sections 3.3. and 4.1.).

Overall, our results suggest that HFST should be stored alongside LAST in large databases, such as national soil information systems. Moreover, HFST should not be corrected *a posteriori* when LAST is known on the same sample because these two parameters provide different information. However, the storage of the two kinds of information in large databases makes it possible to increase the density of information and make better use of the HFST acquired in the field.

5. Conclusion

Here we have shown that trained and professional soil surveyors can predict soil texture classes with higher accuracy than previously stated in the literature. This result is attributed to experienced surveyors who know the pedogenic context of their studied area well and conduct collaborative fieldwork with neighbouring regions. When looking at each field texture class, most of these predictions were consistent. Nevertheless, the extreme texture classes located at the corners of the triangles were much better predicted than those located at the centre of the soil texture triangle. We were able to identify some factors accounting for the observed inconsistencies between hand-feel and laboratory soil texture classes. Our main findings demonstrated a large effect of the size of sand particles, especially for very fine sand (50-100 µm) and very coarse sand (1000-2000 µm), which advocates for detailed fractionation of sand fractions in the laboratory measurements. To our present knowledge, this is the first study that explores in a systematic way biases on HFST due to detailed sand fraction distribution.

We showed that it is possible to calculate a joint probability distribution function of the laboratory measurements of clay, silt, and sand content of each HFST class. This allows us to derive the probabilities of samples belonging to a given field texture class to a given particle-size distribution range.

Finally, we simulated the consequences of using particle-size distribution estimated from hand-feel texture on a pedotransfer function for water retention. Results were consistent with those obtained with the original PTF. Our results also suggest that further research is needed to better explain the roles of clay mineralogy and organic matter and their relationships on CEC and water retention.

Overall, these results are promising for the usefulness of hand-feel texture information in soil databases. Current ongoing studies are being conducted to assess the value of this information for improving digital soil mapping predictions and evaluating the performance of global soil map predictions at finer scales.

Acknowledgments

Most of the soil data were gathered during soil surveys conducted under the programme “Inventaire, Conservation et Gestion des Sols”, partly funded by the French Ministry in charge of Agriculture and other programmes (Carte des sols de la Région Centre) and fundings (INRAE, Régions, Départements, Agences de bassin, Chambres d’Agriculture, etc.). We thank all these organizations and all the soil surveyors for sampling, describing soils, and providing data to the national DoneSol database. We are grateful to the “Groupement d’Intérêt Scientifique Sol”, for his support to the national French Soil Information System. D.A. is coordinator, B.M., P.R. and Z.L. are members, and A.R.-de-F. and H.B. are collaborators of the Research Consortium GLADSOILMAP, supported by LE STUDIUM Loire Valley Institute for Advanced studies through its LE STUDIUM Research Consortium Programme. We thank the editor and the two anonymous reviewers for their helpful comments.

References

AFES, 2008. Référentiel Pédologique. Baize, D., and Girard, M.C. (coord.). Association Française pour l’Etude du Sol. Editions Quae, Paris, France, 405 p. [in French].

AFNOR, 1999. Qualité des sols - Méthodes chimiques - Détermination de la capacité d'échange cationique (CEC) et des cations extractibles. NF X31-130. Association Française de Normalisation. [in French] https://www.boutique.afnor.org/norme/nf-x31-130/qualite-des-sols-methodes-chimiques-determination-de-la-capacite-d-echange-cationique-cec-et-des-cations-extractibles/article/757208/fa049698

AFNOR, 2003. Qualité du sol - Détermination de la distribution granulométrique des particules du sol - Méthode à la pipette. NF X 31–107. Association Française de Normalisation. [in French] https://www.boutique.afnor.org/norme/nf-x31-107/qualite-du-sol-determination-de-la-distribution-granulometrique-des-particules-du-sol-methode-a-la-pipette/article/721991/fa124875

Akamigbo, F., 1984. The accuracy of field textures in a humid tropical environment. Soil survey and land evaluation, 4, 63-70.

Al Majou, H., Bruand, A., Duval, O., Cousin, I., 2007. Variation of the water retention properties of soils: validity of class-pedotransfer functions. Comptes Rendus Geosciences, 339, 632–639.

Amirian-Chakan., Minasny, B., Taghizadeh-Mehrjardi, R., Akbarifazli, R., Darvishpasand, Z., Khordehbin, S., 2019. Some practical aspects of predicting texture data in digital soil mapping. Soil and Tillage Research, 194, 104289.

Arrouays, D., Leenaars, J.G.B., Richer-de-Forges, A.C., Adhikari, K., Ballabio, C., Greve, M., Grundy, M., Guerrero, E., Hempel, J., Hengl, T., Heuvelink, G., Batjes, N., Carvalho, E., Hartemink, A., Hewitt, A., Hong, S.-Y., Krasilnikov, P., Lagacherie, P., Lelyk, G., Libohova, Z., Lilly, A., McBratney, A., McKenzie, N., Vasquez, G.M., Mulder, V.L., Minasny, B., Montanarella, L., Odeh, I., Padarian, J., Poggio, L., Roudier, P., Saby, N., Savin, I., Searle, R., Solbovoy, V., Thompson, J., Smith, S., Sulaeman, Y., Vintila, R., Rossel, R.V., Wilson, P., Zhang, G.-L., Swerts, M., Oorts, K., Karklins, A., Feng, L., Ibelles Navarro, A.R., Levin, A., Laktionova, T., Dell'Acqua, M., Suvannang, N., Ruam, W., Prasad, J., Patil, N., Husnjak, S., Pásztor, L., Okx, J., Hallett, S., Keay, C., Farewell, T., Lilja, H., Juilleret, J., Marx, S., Takata, Y., Kazuyuki, Y., Mansuy, N., Panagos, P., Van Liedekerke, M., Skalsky, R., Sobocka, J., Kobza, J., Eftekhari, K., Alavipanah, S.K., Moussadek, R., Badraoui, M., Da Silva, M., Paterson, G., Gonçalves, M. da C., Theocharopoulos, S., Yemefack, M., Tedou, S., Vrscaj, B., Grob, U., Kozák, J., Boruvka, L., Dobos, E., Taboada, M., Moretti, L., Rodriguez, D., 2017. Soil legacy data rescue via GlobalSoilMap and other international and national initiatives. GeoResJ., 14, 1–19. https://doi.org/10.1016/j.grj.2017.06.001

Arrouays, D., McBratney, A.B., Bouma, J., Libohova, Z., Richer-de-Forges A.C., Morgan, C., Roudier, P., Poggio, L., Mulder V.L., 2020. Impressions of digital soil maps: the good, the not so good, and making them ever better. Geoderma Regional, 20, e00255.

Arrouays, D., Saby, N.P.A., Thioulouze, J., Jolivet, C., Boulonne, L., Ratié, C., 2011. Large trends in French topsoil characteristics are revealed by spatially constrainted multivariate analysis. Geoderma, 161, 107-114.

Arrouays, D., Saby, N.P.A., Walter, C., Lemercier, B., Schvartz, C., 2006. Relationships between particle size distribution and organic carbon in French arable topsoils. Soil Use and Management, 22, 48-51.

Arrouays, D., Vion, I., Kicin, J.L., 1995. Spatial analysis and modeling of topsoil carbon storage in forest humic loamy soils of France. Soil Science, 159, 191-198.

Arya, L M., Leij, F J., Shouse, P J., van Genuchten, M T., 1999. Relationship between the hydraulic conductivity function and the particle-size distribution. Soil Sci. Soc. Am. J., 63, 1063–1070.

Atterberg, A., 1905. Die Rationalle Klassifikation der Sande und Kiese. Chemiker Zeitung, 29, 195-198.

Ashworth, J., Keyes, D., Kirk, R., Lessard, R., 2001. Standard procedure in the hydrometer method for particle size analysis. Communications in Soil Science and Plant Analysis 32, 633–642. https://doi.org/10.1081/CSS-100103897

Baize, D., 1993. Soil science analyses: a guide to current use. Chichester; New York, John Wiley, 192 p.

Bertran, P., Liard, M., Sitzia, L., Tissoux, H., 2016. Map of Pleistocene aeolian deposits in Western Europe, with special emphasis on France, Journal of Quaternary Science, 31 (8), 844-856.

Blume, H.-P., Felix-Henningsen, P., Fischer, W., Frede, H.-G., Guggenberger, G., Horn, R., Stahr, K., (eds.)., 2014. Handbuch der Bodenkunde. Wiley-VCH, Weinheim, Germany, 3584 p. [in German]

Bouma, J., 1989. Using soil survey data for quantitative land evaluation. Advances in Soil Science, 9, 177-213.

Briggs, L.J., McLane, J.W., 1907. The moisture equivalent of soils. USDA Bureau of Soils Bulletin 45, 1–23.

Bruand, A., Duval, O., Cousin, I., 2004. Estimation des propriétés de rétention en eau des sols à partir de la base de données SOLHYDRO: Une première proposition combinant le type d'horizon, sa texture et sa densité apparente. Etude et Gestion des Sols, 11(3), 3-323. [in French]

Bruand, A., Pérez Fernandez, P., Duval, O., 2006. Use of class pedotransfer functions based on texture and bulk density of clods to generate water retention curves. Soil Use and Management, 19, (3) 232–242.

Buchan, G.D., 1989a. Applicability of the Simple Lognormal Model to Particle-size Distribution in Soils. Soil Science, 147 (3), 155–161.

Buchan, G.D., 1989b. Comments on "A Unifying Quantitative Analysis of Soil Texture: Improvement of Precision and Extension of Scale". Soil Sci. Soc. Am. J., 53, 594.

Burke, I.C., Yonker, C.M., Parton, W.J., Cole, C.V., Flach, K., Schimel, D.S., 1989. Texture, climate, and cultivation effects on soil organic matter content in U.S. grassland soils. Soil Sci. Soc. Am. J. 53, 800–805.

Carlile, P., Bui, E., Moran, C., Minasny, B., McBratney, A.B., 2001. Estimating soil particle size distributions and percent sand, silt and clay for six texture classes using the Australian Soil Resource

Information System point database. CSIRO Land and Water Technical Report 29/01: Canberra. Australia.

CRGCST, 2001. Chinese soil taxonomy. Cooperative Research Group on Chinese Soil Taxonomy, Beijing and New York, USA, Science Press.

Chen, S., Arrouays, D., Angers, D.A., Chenu, C., Barré, P., Martin, M.P., Saby N.P.A., Walter, C., 2019. National estimation of soil organic carbon storage potential for arable soils: a data-driven approach coupled with carbon-landscape zones. Sci. Tot. Env., 666, 355-367.

Chen, S., Richer-de-Forges, A.C., Saby, N.P.A., Martin, M.P., Walter, C., Arrouays, D., 2018. Building a pedotransfer function for soil bulk density on regional dataset and testing its validity over a larger area. Geoderma, 312, 52-63.

Chen, S., Richer-de-Forges, A.C., Mulder, V.-L., Martelet, G., Loiseau, T., Lehmann, S., Arrouays, D., 2021. Digital mapping of the soil thickness of loess deposits over a calcareous bedrock in central France. CATENA, 198, 105062.

Chrétien, J., 1971. An attempt to characterize sands by considering them as mineral soil skeletons. Annales Agronomiques, 22(6), 615-654.

Chrétien, J., Bisdom, E.B.A., 1983. The development of soil porosity in experimental sandy soils with clay and mixtures as examined by Quantimet-720 from Besi and by other techniques. Geoderma, 30, 285-302.

Cohen, J., 1960. A coefficient of agreement for nominal scales. Educational & Psychological Measurement, 20, 37–46.

Congalton, R.G., Green, K., 2008. Assessing the Accuracy of Remotely Sensed Data: Principles and Practices. CRC Press, Bocan Raton, FL, USA.

David, O.O., 1999. Improvement in Field Texture Accuracy for Sustainable Agriculture. Journal of Sustainable Agriculture 15, 61–68. https://doi.org/10.1300/J064v15n02_07

Davidson, E.A., Lefebvre, P.A., 1993. Estimating regional carbon stocks and spatially covarying edaphic factors using soil maps at three scales. Biogeochemistry, 22, 107–131.

dos Santos, H.G., Jacomine, P.K.T., dos Anjos, L.H.C., de Oliveira, V.A., Lumbreras, J.F., Coelho, M.R., de Almeida, J.A., de Araujo Filho, J.C., de Oliveira, J.B., Cunha, T.J.F., 2018. Brazilian Soil Classification System, 5th ed. rev. and exp. ed. Brasília, DF: Embrapa, 2018. Embrapa, Brazil, 303 p.

FAO/IIASA/ISRIC/ISS-CAS/JRC, 2008. Harmonized World Soil Database (version 1.0). FAO, Rome, Italy and IIASA, Laxenburg, Austria. 37 p. http://www.fao.org/uploads/media/Harm-World-Soil-DBv7cv_1.pdf (last access 06/28/2021).

Foss, J.E., Wright, W.R., Coles, R.H., 1975. Testing the accuracy of field textures. Soil Sci. Soc. Am. Proc., 39, 800–802.

Franzmeier, D.P., Owens, P.R., 2008. Soil Texture Estimates: A Tool to Compare Texture-by-Feel and Lab Data. Journal of Natural Resources and Life Sciences Education 37, 111–116.

Gori, U., 1994. The pH influence on the index properties of clays. Bulletin of the International Association of Engineering Geology, 50, 37-42.

Gupta, S., Larson, W.E., 1979. Estimating soil water retention characteristics from particle-size distribution, organic matter percent, and bulk density. Water Resources Research, 15(6), 1633–1635.

Hall, D.G.M., Reeve, M.J., Thomasson, A.J., Wright, V.F., 1977. Water retention, porosity, and density of field soils. Soil Survey Tech. Monogr., Rothamsted Experimental Station, Harpenden, England. 9, 1–67.

Hardy, M., 1992. X-ray diffraction measurement of the quartz content of clay and silt fractions in soils. Clay minerals, 27(1), 47-55.

Hardy, M., 1993. Influence of geogenesis and pedogenesis on clay mineral distribution in northern Vietnam soils. Soil Science, 156(5), 336-345.

Hardy, M., Jamagne, M., Elsass, F., Robert, M., Chesneau, D., 1999. Mineralogical development of the silt fractions of a Podzoluvisol on loess in the Paris Basin (France). European Journal of Soil Sci., 50(3), 443-456.

Hassink, J., 1994. Effects of soil texture and grassland management on soil organic C and N and rates of C and N mineralization. Soil Biol. Biochem., 26, 1221–1231.

Hassink, J., 1997. The capacity of soils to preserve organic C and N by their association with clay and silt particles. Plant and Soil, 191, 77–87.

Hewitt, A.E., 2010. New Zealand soil classification. Manaaki Whenua Press, Lincoln, New Zealand.

Hodgson, J., Hollis, J., Jones, R., Palmer, R., 1976. A comparison of field estimates and laboratory analyses of the silt and clay contents of some West Midland soils. J. Soil Sci., 27, 411–419.

Hughes, P., McBratney, A.B., Huang, J., Minasny, B., Michéli, E. and Hempel, J., 2017. Comparisons between USDA Soil Taxonomy and the Australian Soil Classification System I: Data harmonization, calculation of taxonomic distance and inter-taxa variation. Geoderma, 307, pp.198-209.

International Society of Soil Science, 1929. Minutes of the first commission meetings, International Congress of Soil Science. Transactions of the First Commission of the International Society of Soil Science, 4, 215–220.

Isbell, R., 2016. The Australian soil classification. CSIRO publishing. https://ebooks.publish.csiro.au/content/australian-soil-classification-9781486314782#tab-info (last accessed 09/13/2021).

IUSS Working Group WRB, 2015. World Reference Base for Soil Resources 2014, update 2015. International soil classification system for naming soils and creating legends for soil maps. World Soil Resources Reports, No. 106. FAO, Rome. 181 p.

Jamagne, M., 1967. Bases et techniques d'une cartographie des sols. Annales agronomiques, 18, numéro hors série. 142 p. [in French]

Joly, D., Brossard, T., Cardot, H., Cavailhes, J., Hilal, M., Wavresky, P., 2010. Les types des climats en France, une construction spatiale. Les types de climats en France, une construction spatiale. Cybergeo: Revue européenne de géographie / European journal of geography, CNRS-UMR Géographie-cités 8504. Document 501,1-23. [in French] (available on line: https://doi.org/10.4000/cybergeo.23155, last access 06/19/2021)

Kidd, D., Searle, R., Grundy, M., McBratney, A.B., Robinson, N., O'Brien L., Zund, D., Arrouays, D., Thomas, M., Padarian, J., Jones, E., McLean Bennett, J., Minasny, M., Holmes, K., Malone, B., Liddicoat, C., Meier E.A., Stockmann, U., Wilson, P., Wilford, J., Payne, J., Ringrose-Voase, A., Slater, B., Odgers, N., Gray, J., Van Gool, D., Andrews, K., Harms, B., Stower, L., Triantafillis, J., 2020. Operationalising Digital Soil Mapping - Lessons from Australia. Geoderma Regional, 23, e00335.

King, D., Daroussin, J., Tavernier, R., 1994. Development of a soil geographic database from the soil map of the European Communities. CATENA, 21(1), 37-51.

Kuhn, M., 2008. Caret package. J. Stat. Softw., 28, 1–26.

Kowalkowski, A., Truszkowska, R., Borzykowski, J., 1994. Mapa regionów morfogenetycznoglebowych Polski w skali 1:500,000. Prace Komisji Naukowych PTG VIII-15, Warszawa, Poland [in Polish].

Krogh, L., Breuning, H., Greve, M.H., 2000. Cation exchange capacity pedotransfer function for Danish soils. Acta Agric. Scand., Sect. B, Soil and Plant Sci., 50, 1–12.

Kruse, K., (coord.) 2016. Bodenatlas Deutschland. Böden in thematischen Karten; Hrsg.: Bundesanstalt für Geowissenschaften und Rohstoffe (BGR). 144 p. 48 maps. BGR Geozentrum Hannover, Germany [in German].

Lagatu, H., 1905. Classification et nomenclature des terres arables d'après leur constitution mécanique. Compte rendu de l'académie des sciences (France), 1358-1361. [in French].

Levi, M.R., 2017. Modified centroid for estimating sand, silt, and clay from soil texture class. Soil Sci. Soc. Am. J., 81, 578-588.

Libohova, Z., Seybold, C., Wills, S., Beaudette, D., Peaslee, S., Lindbo, D., Adhikari, K., Owens, P.R., 2019. The anatomy of uncertainty for soil pH measurements and predictions: Implications for modelers and practitioners. European Journal of Soil Science, 70, 185-199, doi: 10.1111/ejss.12770

Levine, S., Post, D.F., Ellsworth, T., 1989. An evaluation of student proficiency in field estimation of soil texture. J. Agron. Educ., 18:100–104.

Ma, Y., Minasny, B., Malone, B.P. and Mcbratney, A.B., 2019. Pedology and digital soil mapping (DSM). European Journal of Soil Science, 70(2), pp.216-235.

Ma, Z., Redmond, R.L., 1995. Tau coefficients for accuracy assessment of classification of remote sensing data. Photogrammetric Engineering & Remote Sensing, 61(4), 435–439.

Malone, B.P., Searle, R. 2021a. Updating the Australian digital soil texture mapping (Part 1): Re calibration of field soil texture class centroids. Soil Research, doi:10.1071/SR20283

Malone, B.P., Searle, R., 2021b. Updating the Australian digital soil texture mapping (Part 2): spatial modelling of merged field and lab measurements. Soil Research, doi:10.1071/SR20284

McBratney, A.B., Minasny, B., Cattle, S.R., Vervoort, R.W., 2002. From pedotransfer functions to soil inference systems. Geoderma, 109, (1–2), 41-73.

McDonald, R.C., Isbell, R., Speight, J.G., Walker, J., Hopkins, M., 1998. Australian soil and land survey: Field handbook. CSIRO publishing, Clayton, Australia.

Michéli, E., Láng, V., Owens, P.R., McBratney, A. and Hempel, J., 2016. Testing the pedometric evaluation of taxonomic units on soil taxonomy—A step in advancing towards a universal soil classification system. Geoderma, 264, pp.340-349.

Minasny, B., McBratney, A.B., 2001. The Australian soil texture boomerang: a comparison of the Australian and USDA/FAO soil particle-size classification systems. Aust. J. Soil Res., 39, 1443–1451.

Minasny, B., McBratney, A.B., 2002. The efficiency of various approaches to estimates of soil hydraulic properties. Geoderma, 107, 55–70.

Minasny, B., McBratney, AB., Field, D.J., Tranter, G., McKenzie, N.J., Brough, D.M., 2007. Relationships between field texture and particle-size distribution in Australia and their implications. Soil Res., 45:428–437.

Moeys, J., Shangguan, W., Petzold, R., Minasny, B., Rosca, B., Jelinski, N., Zelazny, W., Marcondes Silva Souza, R., Safanelli, J.L., ten Caten, A., 2018. Package ‘soiltexture’: Functions for Soil Texture Plot, Classification and Transformation. Version 1.5.1. https://cran.r-project.org/web/packages/soiltexture/soiltexture.pdf

Nemes, A., Wösten, J.H.M., Lilly, A., Oude Voshaar, J.H., 1999. Evaluation of different procedures to interpolate particle-size distributions to achieve compatibility within soil databases. Geoderma, 90, 187–202.

NRCS-USDA, 2012. Field book for describing and sampling soils, Version 3.0. National Soil Survey Center. National resources Conservation service. U.S. Department of Agriculture. Lincoln, NE, USA.

Ogunkunle, A.O., 1993. Soil in land suitability evaluation: an example with oil palm in Nigeria. Soil Use & Management 9, 35–39. https://doi.org/10.1111/j.1475-2743.1993.tb00925.x

Pachepsky, Y.A., Rawls, W.J., 1999. Accuracy and Reliability of Pedotransfer Functions as Affected by Grouping Soils. Soil Sci. Soc. Am. J. 63, 1748–1757. https://doi.org/10.2136/sssaj1999.6361748x

Pachepsky, Y.A., Rawls, W.J., Lin, H.S., 2006. Hydropedology and pedotransfer functions. Geoderma 131, 308–316. https://doi.org/10.1016/j.geoderma.2005.03.012

Piedallu, C., Gegout, J.C., Bruand, A., Seynave, I., 2011. Mapping soil water holding capacity over large areas to predict potential production of forest stands. Geoderma, 160, (3-4), 355-366.

Polish soil classification (Systematyka gleb Polski), 1989. Roczniki Gleboznawcze - Soil Science Annual, 40(3/4): 1-150.

Post, D.F., Huete, A.R., Pease, D.S., 1986. A comparison of soil scientist estimations and laboratory determination of some Arizona soil properties. Journal of Soil and Water Conservation, 41, 421–424.

R Core Team, 2021. R: A language and environment for statistical computing. R Foundation for Statistical Computing, Vienna, Austria. URL https://www.R-project.org/.

Rawls, W.J., Pachepsky, Y.A., 2002. Using field topographic descriptors to estimate soil water retention. Soil Science, 167, 423–435.

Rawls, W.J., Gish, T.J., Brakensiek, D.L., 1991. Estimating soil water retention from soil physical properties and characteristics. Advances in Soil Science, 16, 213–234.

Rehman, H.U., Knadel, M., de Jonge, L.W., Moldrup, P., Greve, M.H., Arthur, E., 2019. Comparison of cation exchange capacity estimated from Vis–NIR spectral reflectance data and a pedotransfer function. Vadose Zone Journal, 18(1), [180192].

Revelle, W., 2011. psych: Procedures for Psychological, Psychometric, and Personality Research. Version 1.7.5. Northwestern Univ., Evanston, IL. Available from: https://cran.r-project.org/package=psych. (last access 07/15/2021).

Richer-de-Forges, A.C., Arrouays, D., Feller, C., Jamagne, M., 2008. Perdus dans le triangle des textures. Etude et Gestion des Sols, 15(2), 97-111. [in French].

Richer-de-Forges, A.C., Baffet, M., Berger, C., Coste, S., Courbe, C., Jalabert, S., Lacassin, J.-C., Maillant, S., Michel, F., Moulin, J., Party, J.-P., Renouard, C., Sauter, J., Scheurer, O., Verbèque, B., Desbourdes, S., Héliès, F., Lehmann, S., Saby N.P.A., Tientcheu, E., Jamagne M., Laroche, B., Bardy, M., Voltz, M., 2014. La cartographie des sols à moyennes échelles en France métropolitaine. Etude et Gestion des Sols, 21(1), 25-36. [in French]

Ritchey, E.L., McGrath, J.M., Gehring, D., 2015. Determining Soil Texture by Feel. Agriculture and Natural Resources Publications. 139. University of Kentucky, College of Agriculture, Food and Environment, Lexington, KY, 40546, USA.

Robert, M., Hardy, M., Elsass, F., 1991. Crystallochemistry, properties and organization of soil clays derived from major sedimentary rocks in France. Clay minerals, 26(3), 409-420.

Robinson, N., Benke, K., Norng, S., 2015. Identification and interpretation of sources of uncertainty in soils change in a global systems-based modelling process. Soil Research Internal report. CSIRO, Canberra, Australia.

Román Dobarco, M., Bourennane, H., Arrouays, D., Saby, N.P.A., Cousin, I., Martin, M.P., 2019a. Uncertainty assessment of *GlobalSoilMap* soil available water capacity products: a French case study. Geoderma, 344, 14-30.

Román Dobarco, M., Cousin, I., Le Bas, C., Martin, M.P., 2019b. Pedotransfer functions for predicting available water capacity in French soils, their applicability domain and associated uncertainty. Geoderma, 336, 81-95.

Román Dobarco, M., Orton, T.G., Arrouays, D., Lemercier, B., Paroissien, J.B., Walter, C., Saby, N.P.A., 2016. Prediction of soil texture in agricultural land using summary statistics and area-to-point kriging in Region Centre (France), Geoderma Regional, 7(3), 279-292.

Rossiter, D.G., 2004.Technical Note: Statistical methods for accuracy assessment of classified thematic maps. Department of Earth Systems Analysis. International Institute for Geo-information Science & Earth Observation (ITC), Enschede, The Netherlands, 46 p. Available on line at: https://www.researchgate.net/publication/228802780_Technical_Note_Statistical_methods_for_accuracy_assesment_of_classified_thematic_maps. (Last access 07-21-2021).

Rossiter, D.G., Liu, J, Carlisle, S., Zhu, A.-X., 2015. Can citizen science assist digital soil mapping? Geoderma, 259:71–80.

Rousseva, S.S., 1997. Data transformations between soil texture schemes. European Journal of Soil Science, 48, 749-758.

Rudiyanto, Minasny, B., Chaney, N.W., Maggi, F., Goh Eng Giap, S., Shah, R.M., Fiantis, D., Setiawan, B.I., 2021. Pedotransfer functions for estimating soil hydraulic properties from saturation to dryness. Geoderma 403, 115194. https://doi.org/10.1016/j.geoderma.2021.115194

Ryżak, M., Bieganowski, A., 2011. Methodological aspects of determining soil particle-size distribution using the laser diffraction method. Journal of Plant Nutrition and Soil Science 174, 624–633. https://doi.org/10.1002/jpln.201000255Salley, S.W., Herrick, J.E., Holmes, C.V., Karl, J.W., Levi, M.R., McCord, S.E., van de Waal, C., Van Zee, J.W., 2018. A Comparison of Soil Texture-by-Feel Estimates: Implications for the Citizen Soil Scientist. Soil Sci. Soc. Am. J., 82, 1526–1537.

Salter, P.J., Berry, G., Williams, J.B., 1966. The influence of texture on the moisture characteristics of soils: III. Quantitative relationships between particle size, composition and available water capacity. Journal of Soil Science, 17, 93–98.

Salter, P.J., Williams, J.B., 1969. The influence of texture on the moisture characteristics of soils: V. Relationships between particle-size composition and moisture contents at the upper and lower limits of available water. Journal of Soil Science, 20, 126–131.

Searle, R., McBratney, A.B., Grundy, M., Kidd, D., Malone, B., Arrouays, D., Stockman, U, Zund, P, Wilson, P, Wilford P, Van Gool D., Triantafilis, J., Thomas, M., Stower, E., Slater, B., Robinson, N., Ringrose-Voase, A., Padarian, J., Payne, J., Orton, T.G., Odgers, N., O'Brien, L., Minasny, B., Meier, E., McLean Bennett, J., Liddicoat, C., Jones, E., Holmes, K., Harms, B., Gray., J, Bu, E., 2021. Digital Soil Mapping and Assessment for Australia and Beyond: A Propitious Future. Geoderma Regional, 24, e00339.

Shirazi, M. A., Boersma, L., 1984. A Unifying Quantitative Analysis of Soil Texture. Soil Science Society of America Journal, 48 (1), 142–147.

Shirazi, M.A., Boersma, L., Hart, W.A., 1988. Unifying Quantitative Analysis of Soil Texture: Improvement of Precision and Extension of Scale. Soil Science Society of America Journal 52 (1), 181–190.

Shishov, L.L., Tonkonogov, V.D., Lebedeva, I.I., Gerasimova, M.I., (eds.). 2004. Classification and Diagnostics of Soils of Russia. Smolensk, Oecumena, 343 pp. [in Russian].

Sponagel, H., Grottenthaler,W., Hartmann, K.J., Hartwich, R., Janetzko, P., Joisten, H., Kühn, D., Sabel, K.J., Traidl, R. (Eds.), 2005. Bodenkundliche Kartieranleitung (German Manual of Soil Mapping, KA5), fifth ed. Bundesanstalt für Geowissenschaften und Rohstoffe, Hannover, Germany [*in German*].

Stokes, G.G., 1851. On the effect of internal friction of fluids on the motion of pendulums. Transactions of the Cambridge Philosophical Society, 9, part ii, 8–106.

Takahashi, T., Nakano, K., Nira, R., Kumagai, E., Nishida, M, Namikawa, M., 2020. Conversion of soil particle-size distribution and texture classification from ISSS system to FAO/USDA system in Japanese paddy soils. Soil Science and Plant Nutrition, 66(3), 407-414.

Thien, S.J., 1979. A flow diagram for teaching texture by feel analysis. Journal of Agronomic Education, 8, 54-55.

USDA-NRCS, 2014. Keys to soil taxonomy. 12th edition. United States Department of Agriculture, National Resources Conservation Service, Lincoln, NE, USA, 359 p.

Van Looy, K., Bouma, J., Herbst, M., Koestel, J., Minasny, B., Mishra, U., Montzka, C., Nemes, A., Pachepsky, Y.A., Padarian, J., Schaap, M.G., Toth, B., Verhoef, A., Vanderborght, J., van der Ploeg, M.J., Weihermuller, L., Zacharias, S., Zhang, Y.G., Vereecken, H., 2017. Pedotransfer Functions in Earth System Science: Challenges and Perspectives. Reviews of Geophysics, 55, 4, 1199-1256.

Veihmeyer, F.J., Hendrickson, A.H., 1927. Soil-moisture conditions in relation to plant growth. Plant Physiol., 2, 71–82. https://doi.org/10.1104/pp.2.1.71

Voinchet, P., Despriee, J., Tissoux, H., Falgueres, C., Bahain, J.J., Gageonnet, R., Depont, J., Dolo, J.M., 2010. ESR chronology of alluvial deposits and first human settlements of the Middle Loire Basin (Region Centre, France). Quat. Geochronol., 5 (2–3) 381-384.

Vos, C., Don, A., Prietz, R., Heidkamp, A., Freibauer, A., 2016. Field-based soil-texture estimates could replace laboratory analysis. Geoderma, 267, 215–219.

Wickham, H., 2009. ggplot2: Elegant Graphics for Data Analysis. Springer New York, New York, NY. https://doi.org/10.1007/978-0-387-98141-3

Wösten, J.H.M., Finke, P.A., Jansen M.J.W., 1995. Comparison of class and continuous pedotransfer functions to generate soil hydraulic characteristics. Geoderma, 66, 227–237.

Wösten, J.H.M., Lilly, A., Nemes, A., Le Bas, C., 1999. Development and use of a database of hydraulic properties of European soils. Geoderma, 90, 169–185

Wösten, J.H.M., Pachepsky, Y.A., Rawls, W.J., 2001. Pedotransfer functions: bridging gap between available basic soil data and missing soil hydraulic characteristics. Journal of Hydrology, 251, 123–150.

Yaalon, D., 1989. Comments on "A Unifying Quantitative Analysis of Soil Texture". Soil Sci. Soc. Am. J., 53, 595.